

Study on the Calculation of Vacuum Temperature Field of Dual Redundancy Permanent Magnet Synchronous Motor

Zhao Li

Chongqing Vocational College of Transportation, Chongqing, China

zhaolicq@126.com

Keywords: Double redundancy, Permanent magnet synchronous motor, Three dimensional temperature field, Loss

Abstract: This paper introduces a kind of low thermal coupling non electromagnetic coupling dual redundancy permanent magnet synchronous motor Through the finite element analysis of two-dimensional electromagnetic field, the copper loss of stator winding, the iron loss of big teeth, small teeth and yoke of stator core, and the eddy current loss of permanent magnet and sheath are obtained, and their heat generation rate is calculated. According to the theory of heat transfer, the thermal conductivity and surface heat transfer coefficient of each component of motor are determined, and the refined modeling of stator winding coil is carried out, and the three-dimensional motor is established Based on the temperature field model, the three-dimensional global steady-state temperature distribution of the motor under rated condition is obtained by finite element analysis. When one set of winding has single-phase short circuit fault and the other set of winding works separately, the maximum temperature difference between the fault phase winding and the working winding is 7.1, the results show that the thermal coupling between the phase windings is relatively low. When two sets of windings work at the same time, the error between the analysis result and the experimental result of the highest temperature of the shell surface is 4.5%, which proves the validity of the analysis method

1. Introduction

Dual redundancy permanent magnet synchronous motor (Motor, drpmsm) is not only of high power density, but also of high reliability and safety. It will be widely used in the aerospace industry. In the aerospace field, it not only pays attention to the overall operation performance of redundant motor, but also pays more attention to the impact of temperature rise on the system safety. In recent years, the research on the temperature field inside the motor is quite good at home and abroad For the sake of rapidity, the modeling method of temperature field is studied in the literature. The analysis of temperature field of PMSM is mainly to consider the demagnetization phenomenon of permanent magnet material under high temperature. At present, the analysis of temperature field of motor is mostly aimed at the model of large or special motor. The literature studies the temperature field distribution of a certain element of motor. But for the whole area temperature field of dual redundancy PMSM The research is very few. In this paper, a kind of non-electromagnetic coupling low thermal coupling dual redundancy permanent magnet synchronous motor proposed by the author is used to establish the steady-state global temperature field model of the motor by using the finite element analysis software, and the analysis and calculation are carried out. Under the normal condition, the two sets of motor windings work together - under the dual redundancy working mode and one set of winding has phase short-circuit fault Another set of winding work - three-dimensional temperature field distribution in single redundancy mode. The analysis and experimental results show that the new dual redundancy PMSM has low inter phase thermal coupling.

2. A New Dual Redundancy Permanent Magnet Synchronous Motor

The structure of the new dual redundancy permanent magnet synchronous motor proposed in this

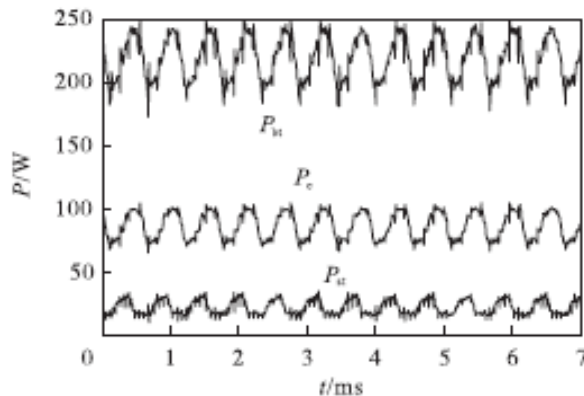
3.1 Copper Consumption of Stator Winding

According to Joule Lenz law, the basic copper consumption of polyphase winding motor is

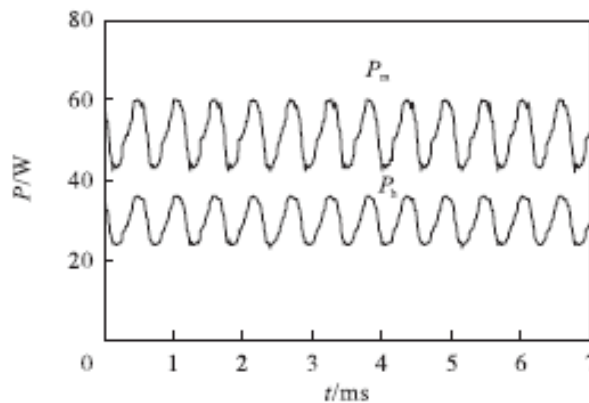
$PCU = \sum i^2 r$ (1), where: I is the effective value of current in winding x , a ; R It is the resistance value of the winding under the working temperature, Ω . Starting from the constant overall copper consumption of the motor, the rated current of the phase winding when a set of winding works alone is times of the rated current of the phase winding when two sets of winding work together; the rated power when two sets of winding work together is times of the rated power when one set of winding works alone. When a certain phase of the motor has a short circuit fault, the set of y -winding to which the phase belongs the group stops working, and the normal set of winding still works. The non-fault phase winding of the fault set is open circuit, and the fault short circuit current of the fault phase winding $i_f = EF / (\omega LF)$ (2). In the formula, EF is the permanent magnetic induction electromotive force inside the fault part of winding, V ; ω is the electric angle frequency, rad / S ; LF is the corresponding inductance of the fault part of winding, H .

3.2 Iron Loss and Eddy Current Loss

In this paper, the two-dimensional electromagnetic field simulation is used to obtain all kinds of losses as the heat source of the temperature field. The magnetic density of the big teeth, the small teeth and the yoke of the stator core are quite different. In order to accurately calculate the loss of the stator core, they are considered separately. When two sets of windings are working at the rated speed and only one set of windings is working separately, the loss of the stator core and the yoke PE, the loss of the big teeth PBT, the loss of the small teeth PST The curves of PM eddy current loss of permanent magnet and pH eddy current loss of sheath with time are shown in Fig. 2 and Fig. 3 respectively.

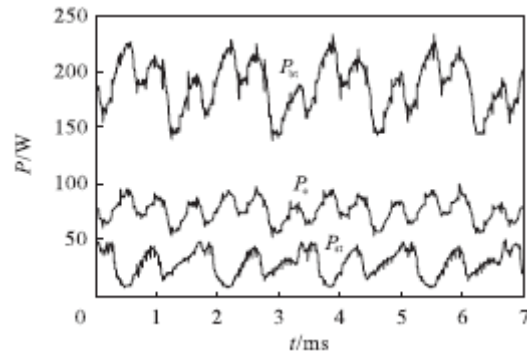


(a) Stator iron loss

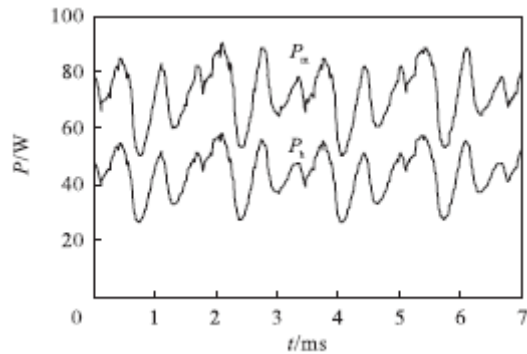


(b) Eddy current loss on permanent magnet and sheath

Fig.2 Loss of Motor under Double Redundancy Operation with Rated Load



(a) Stator iron loss



(b) Eddy current loss on permanent magnet and sheath

Fig.3 Loss of Motor with 0.7 Times Rated Load and Single Redundancy

According to the volume of each component, the heat generation rate (referred to as heat source density in thermodynamics) of each component in steady state is obtained according to the loss of each component obtained from the above analysis, as shown in Table 1

Table 1 Average Loss and Heat Generation Rate of Each Part of Motor under Rated Working Condition

Motor components	Dual redundancy operation mode		Single redundancy mode	
	Loss(W)	Heat generation rate (W/m ³)	Loss(W)	Heat generation rate (W/m ³)
Stator yoke	86.67	2.689×10^5	76.47	2.373×10^5
Stator big teeth	218.51	6.906×10^5	187.19	5.916×10^5
Stator denticle	22.29	7.148×10^5	28.87	9.256×10^5
Permanent magnet	29.81	2.492×10^5	43.61	3.646×10^5
Sheath	51.62	6.197×10^6	72.02	8.645×10^6
Rotor core	0.53	4.752×10^3	0.92	8.272×10^3

4. Calculation Basis of Temperature Field

In the three-dimensional temperature field solution, in order to simplify the analysis, the following assumptions are made: 1) after painting, the surface of the thermal insulation material is flat; 2) the parts are well processed, and the contact thermal resistance between the sheath, magnetic steel, rotor and shaft, as well as between the shell and the stator core is zero; 3) the heat dissipation coefficient of each part and the air contact surface is taken as the average value.

4.1 Solving Equations and Boundary Conditions

According to the theory of heat transfer, for anisotropic medium, the boundary condition of rectangular coordinate system in the solution area of steady three-dimensional temperature field in

$$\begin{cases} \frac{\partial}{\partial x}(\lambda_x \frac{\partial T}{\partial x}) + \frac{\partial}{\partial y}(\lambda_y \frac{\partial T}{\partial y}) + \frac{\partial}{\partial z}(\lambda_z \frac{\partial T}{\partial z}) + q(x, y, z) = 0 \\ S: -\lambda_x \frac{\partial T}{\partial n} = \alpha(T - T_m) \end{cases} \quad (3)$$

the motor is

Where: T is the temperature of the object, K; X, y and Z are the thermal conductivity coefficients in the X, y and Z directions, w / (m · K); q is the heat source density, w / m³; s is the outer surface and end surface of the motor; α is the heat dissipation coefficient, w / (m · K); T_m is the ambient temperature, K

4.2 Establishment of Equivalent Thermal Model

In order to accurately analyze the temperature distribution in the slot of the motor, the following assumptions will be made: ① the wires in the slot are evenly arranged with uniform heat generation; ② the wires at the end of the motor are evenly arranged; ③ the slot is fully impregnated with paint and evenly distributed; ④ the eddy current loss generated during the operation of the motor is evenly distributed in the sheath and permanent magnet. The refined equivalent thermal model of the slot of the stator winding is shown in Figure 4 Show.

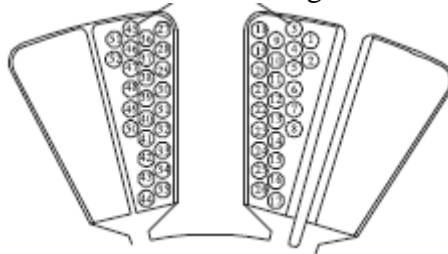


Fig.4 Refined Stator Winding Model

The heat transfer process in the motor includes conduction, convection and radiation 3 the heat transfer process in the motor is directly related to the thermal conductivity and surface heat dissipation coefficient of the medium. Before analyzing the temperature field, first determine the equivalent thermal conductivity and surface heat dissipation coefficient of each component of the motor. The rotation of the rotor of the motor will cause air flow in the air gap, and the air is the flowing fluid, resulting in the temperature the field is coupled with the fluid field. In this paper, the equivalent thermal conductivity (EFF) is introduced, and its heat exchange is equivalent to the heat transfer of the static fluid, that is, the heat transferred by the flowing air in the air gap in unit time is equal to the heat transferred by the equivalent static fluid. The equivalent thermal conductivity at

the air gap is determined according to its Reynolds number $Re = v_{r1} \delta / \nu$ (4) v_{r1} is the linear speed of rotor surface, M / S; ν is the air kinematic viscosity, m² / S; δ is the air gap length, m,

and $\delta = (D_{i1} - D_2) / 2$ (5) d_{i1} is the inner diameter of stator, m; D_2 is the outer diameter of rotor,

$Re < 41.2 \sqrt{D_{i1} / \delta}$ The equivalent thermal conductivity of air gap is the thermal conductivity of

air $Re \geq 41.2 \sqrt{D_{i1} / \delta}$ The air flow in the air gap is turbulent, and its thermal conductivity can be

$$\begin{cases} \lambda_{eff} = 0.0019 \eta^{-0.9084} Re^{0.4614 \ln[333361 \eta]} \\ \eta = D_2 / D_{i1} \end{cases}$$

expressed as (6) In addition, the thickness of the heat insulation board on both sides of the small teeth is 1 m, and its thermal conductivity is 0.2, w / (m · K).

4.3 Determination of Heat Dissipation Coefficient of Fuselage Surface and End

Since there is no fan at the end of the motor, the way of heat dissipation from the shell surface is natural air cooling. The surface heat dissipation coefficient is $\alpha_1 = 9.73 + 14u^{0.62}$ (7) where u is the surface wind speed of the casing, M / s. The heat dissipation coefficient at the end of the stator core

is $\alpha_2 = 15 + 6.5v_{a1}^{0.62}$ (8) The calculation formulas of the heat dissipation coefficient of the end face of the rotor core are as follows $\alpha_2 = Nu_r \lambda_a / (D_2/2)$ (9) $Nu_r = 1.67 Re_r^{0.335}$ (10) $Re_r = \pi D_2^2 n / (120 \gamma)$ (11) Where, α_2 is the heat dissipation coefficient of the end face of the core, $w / (M^2 \cdot K)$; Nu_r is the Nusselt constant of the end face of the core; Re_r is the Reynolds number of the end face of the core; λ_a is the thermal conductivity coefficient of the air, $w / (m \cdot K)$ γ is the dynamic viscosity of the air, $PA \cdot s$.

5. Analysis of Temperature Field Simulation Results

5.1 Temperature Field of Two Sets of Winding Working at the Same Time under Rated Load

Assuming the ambient temperature is 40, °C, the loss results obtained from the analysis of the magnetic field of two sets of motor windings working at the same time under the rated load are substituted into the three-dimensional temperature field solution model to obtain the three-dimensional temperature field distribution of the motor during the steady-state operation. The maximum temperature at the center of the winding end is 121.27, °C. The maximum temperature of the stator core and the shell is 119.14, °C and 106.85 respectively, The temperature of the stator winding is higher than the temperature of the stator core. After the heat shield is placed on both sides of the stator small teeth, the heat transfer capacity is weakened through the small teeth, and the heat is mainly transmitted to the yoke and the shell to the surrounding environment through the big teeth. Because the rotor surface has a sheath, the eddy current loss caused by the tooth harmonic and armature reaction harmonic magnetic field in its internal part, the permanent magnet will also produce some eddy current loss, in addition to skin effect Due to the influence of strain, the surface temperature of permanent magnet is relatively high, and the maximum temperature of permanent magnet and rotor core are 119.41, °C and 118.55, °C, respectively. Due to the long axial length of motor, there is a certain temperature difference between stator and rotor in the axial direction.

5.2 Temperature Field of One Phase Winding Short Circuit Fault While another Set of Winding is working

When the A1 phase winding in Figure 5 has a short circuit fault, the controller cuts off the whole set of A1, B1 and C1 windings where the A1 phase winding is located, and the other set of windings A2, B2 and C2 work separately. The short circuit current of A1 phase is 27, a, and the normal winding current is 2 in = 25, A. As shown in Figure 5, the cloud chart of temperature field distribution when the motor outputs 0.7 times of rated load. It can be seen from Figure 5 that the temperature value of the coil conductor at the center of the slot can be seen compared with the traditional winding equivalent to a copper rod. When the phase A1 has a single-phase short circuit fault, the temperature at the end center of the phase A1 winding is the highest, with the maximum temperature of 151.41, The temperature of the tip of the small teeth and the pole shoe of the big teeth in the stator core are relatively high, and the maximum temperature of the stator core is 135.82, The comparison of the temperature of the coil on the two-phase big teeth of the normal winding B2 and C2 adjacent to the fault phase A1 at the central section of the motor and the coil on the two-phase big teeth of the normal winding A2 far away from the fault phase is shown in Figure 6. The temperature of the conductor in the slot increases first and then decreases along the radius direction. This is because the heat is easily transmitted to the shell through the big teeth and yoke, while the heat dissipation at the center of the slot is the worst the difference of temperature rise between phase B2 and phase A2 is not obvious. Except that the temperature of phase B2 and phase C2 is lower than that of phase A2 due to the slightly better heat dissipation condition of phase B2 and phase C2, the temperature of phase B2 and phase C2 is higher than that of phase A2, and the maximum temperature difference between them is 3.64, The difference between the maximum temperature of phase A1 and that of phase B2 and C2 is 7.10, °C. It can be seen that the existence of small teeth and heat insulation plates on both sides of small teeth has obvious heat insulation

effect, which makes the thermal coupling between adjacent two phases of windings very small.

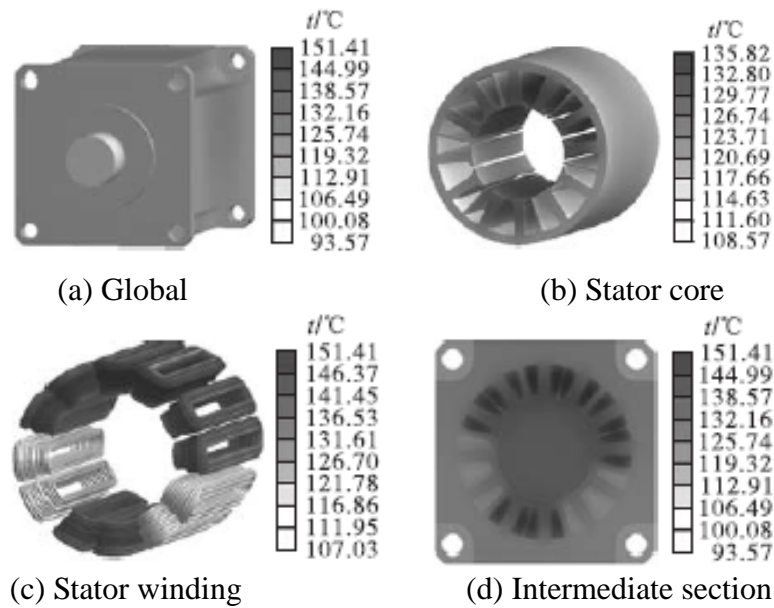


Fig.5 Temperature Field of One Phase Winding Short Circuit Fault under 0.7 Times Rated Load of Motor When the Other Set of Winding Works Separately

Temperature(°C).

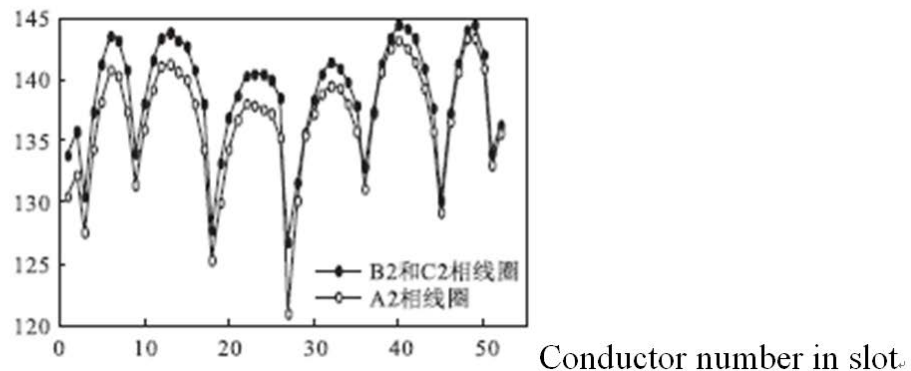


Fig.6 Temperature Comparison of A2 and B2 Phase Working Windings in Case of Single-Phase Short Circuit Fault

6. Experimental Result

A prime mover is used to drive a new type of double redundancy motor to operate as a generator to supply power for two groups of three-phase resistance boxes, and the output current of each phase is rated current, which is used to simulate the rated working condition of the motor. After 2 hours of operation, the surface temperature of the shell tends to be stable. The surface temperature image of the shell is taken with thermacam E30 infrared thermal imager, and the ambient temperature is 23, °C during the experiment. The maximum surface temperature of the shell is 102, the error is 4.5%. It shows that the analysis method is effective.

7. Conclusion

(1) When the temperature of the motor reaches steady state, the temperature of the end of the stator winding is the highest, followed by the center of the winding in the stator slot, and the temperature of the stator winding is significantly higher than the temperature of the stator core. (2) the heat insulation effect of the heat insulation plate is obvious, which can change the direction of the heat flow, so that the heat of the winding is transmitted to the external environment along the

big teeth through the yoke of the stator core and the shell, so as to prevent the fault phase winding from producing in case of short circuit fault The heat generated affects the normal phase winding. (3) The eddy current loss in the rotor sheath is the main loss on the rotor, and the axial segment of the sheath can reduce the loss. (4) The advantage of the refined modeling of the stator winding coil compared with the traditional modeling method is that it can more clearly understand the maximum temperature of the winding. (5) the simulation calculation and experimental results show that the two sets of winding work at the same time and drag the rated value When one set of winding has single-phase short-circuit fault and the other set of winding works alone to drag 0.7 times of rated load, the winding and permanent magnet do not exceed the allowable maximum temperature, so the motor can operate reliably.

References

- [1] Liu Ruifang, Zhu Jian, Cao Junci. Temperature field analysis of permanent magnet synchronous motor for electric vehicle with amorphous and silicon steel stator core [J]. Journal of Beijing Jiaotong University, vol.43, no.5, pp.119-125, 2019.
- [2] LAN Zhiyong, Wang Lin, Xu Chen, et al. Temperature field and water cooling analysis of high speed permanent magnet synchronous motor [J]. Electric drive, vol.48, no.12, pp.81-85, 2018.
- [3] Lu Ling, Wang Shuwang. Global temperature field analysis and water channel optimization design of permanent magnet synchronous motor [J]. Application of motor and control, vol.45, no.5, pp.52-57, 2018.
- [4] Han Xueyan, song Cong. study on temperature rise calculation and influencing factors of permanent magnet synchronous motor for vehicle based on magneto thermal coupling method [J]. Journal of motor and control, vol.24, no.2, pp.28-35, 2020.
- [5] Ding Shuye, Zhu Min, Jiang Xin. Study on three-dimensional temperature field and temperature stress coupling of permanent magnet synchronous motor [J]. Journal of motor and control, vol.22, no.1, pp.53-60, 71, 2018.
- [6] Li Wei Li, Hou Fu Yu, Shen Jia Feng. Study on multi physical field of high speed permanent magnet synchronous motor considering the mechanical strength of rotor sheath and permanent magnet [J]. Journal of Beijing Jiaotong University, vol.43, no.5, pp.110-118, 2019.
- [7] Wang Xiaofei, Dai Ying, Luo Jian. Water channel design and temperature field analysis of vehicle permanent magnet synchronous motor based on fluid solid coupling [J]. Journal of electrical technology, vol.34, no.z1, pp.22-29, 2019.
- [8] Wu Boxi, Wan Zhenping, Zhang Kun, et al. Design of turn back cooling channel for PMSM considering temperature field and flow field [J]. Journal of electrical technology, vol.34, no.11, pp.2306-2314, 2019.